LETTER **Communicated by Alain Destexhe**

Estimation of Time-Dependent Input from Neuronal Membrane Potential

Ryota Kobayashi
kobayashi@cns.ci.ritsumei.ac.jp
Department of Human and Computer Intelligence, Ritsumeikan University, Shiga 525-8577, Japan

Shigeru Shinomoto
shinomoto@scphys.kyoto-u.ac.jp
Department of Physics, Graduate School of Science, Kyoto University, Kyoto 606-8502, Japan

Petr Lansky
lansky@biomed.cas.cz
Institute of Physiology, Academy of Sciences of Czech Republic, 142 20 Prague 4, Czech Republic

The set of firing rates of the presynaptic excitatory and inhibitory neurons constitutes the input signal to the postsynaptic neuron. Estimation of the time-varying input rates from intracellularly recorded membrane potential is investigated here. For that purpose, the membrane potential dynamics must be specified. We consider the Ornstein-Uhlenbeck stochastic process, one of the most common single-neuron models, with time-dependent mean and variance. Assuming the slow variation of these two moments, it is possible to formulate the estimation problem by using a state-space model. We develop an algorithm that estimates the paths of the mean and variance of the input current by using the empirical Bayes approach. Then the input firing rates are directly available from the moments. The proposed method is applied to three simulated data examples: constant signal, sinusoidally modulated signal, and constant signal with a jump. For the constant signal, the estimation performance of the method is comparable to that of the traditionally applied maximum likelihood method. Further, the proposed method accurately estimates both continuous and discontinuous time-variable signals. In the case of the signal with a jump, which does not satisfy the assumption of slow variability, the robustness of the method is verified. It can be concluded that the method provides reliable estimates of the total input firing rates, which are not experimentally measurable.

1 Introduction

Cortical neurons transmit information by transforming synaptic inputs into spikes. Deducing the input from the spiking activity has been at the center of interest for decades. Spike trains of a single neuron or a small group of neurons were recorded in many experiments and often described by theoretical models. For example, the spike trains observed in the visual cortex were compared with those predicted by the models (Softky & Koch, 1993; Shadlen & Newsome, 1995, 1998). These studies suggested that the excitatory and inhibitory inputs are balanced. However, spiking data can provide only indirect means for deducing the input to the neuron. In such data, the dynamics of subthreshold membrane potential are not available, and a clue about the presynaptic activity is potentially hidden in the membrane trajectory. DeWeese and Zador (2006) recorded the membrane potential of a neuron in rat primary auditory cortex *in vivo*. They concluded that the presynaptic activity is highly correlated among neurons, and it varies faster than the mean interspike interval of a neuron. Such a result would hardly be achieved from only spiking data. Thus, we can expect that for analyzing the population activity of presynaptic neurons in more detail, it is necessary to have membrane potential data. For this reason, it would be important to devise a systematic method for estimating presynaptic input signal from these types of data.

In this letter, we propose a method for estimating the time-varying firing rates of the populations of excitatory and inhibitory neurons impinging on the target neuron from which the membrane potential trajectory is experimentally recorded. These firing rates represent the input signal from the point of view of the frequency coding concept. To develop such a statistical procedure, a neuronal model has to be considered. The integrate-and-fire neuronal models are probably the most common one-dimensional mathematical representations of a single neuron (see for a review Burkitt, 2006). In fact, it has been shown (Kistler, Gerstner, & van Hemmen, 1997; Jolivet, Lewis, & Gerstner, 2004; Kobayashi & Shinomoto, 2007) that integrate-and-fire models are a good approximation of the more detailed biophysical models, including the Hodgkin-Huxley model. Therefore, analysis of integrate-and-fire models, despite their relative simplicity, provides a rather reliable prediction of analogous results for more complicated models. For our purpose, we selected Stein's model and its diffusion counterpart, the Ornstein-Uhlenbeck model. Stein's model is introduced because it offers a distinction between its intrinsic parameters and the input signal, a distinction that is not obvious in the Ornstein-Uhlenbeck model, and the role of noise is often misinterpreted. The Ornstein-Uhlenbeck model possesses continuous trajectories, and we assume that a trajectory is sampled and the samples are used to determine the neuronal input.

The estimation problem of a time-varying input signal from a sampled voltage trace is ill posed. The sets of parameters and functions giving rise

to a particular voltage trace are not uniquely determined without additional assumptions. The problem can be formulated as the estimation of a hidden state in a state-space model by assuming that the input signal is slowly varying. This estimation problem appears in various studies on neuronal data analysis, such as spike train analysis (Smith & Brown, 2003; Eden, Frank, Barbieri, Solo, & Brown, 2004; Koyama & Shinomoto, 2005; Shimokawa & Shinomoto, 2009; Paninski et al., 2010), brain-computer interface (Koyama, Chase et al., 2010) and analysis of neuronal imaging data (Friston et al., 2002; Huys & Paninski, 2009). In all these cases, Kalman filtering and smoothing techniques are applied to estimate the hidden state from the observed data (reviewed in Paninski et al., 2010).

In this study, we develop a method for estimating the time-dependent input signal from a subthreshold voltage trace of a neuron described by the Ornstein-Uhlenbeck model. The proposed method is applied to simulated voltage traces, and the estimation precision is evaluated for continuous and discontinuous input signals.

2 Model

The leaky integrate-and-fire concept contains several different models, and we investigate one of them; the Ornstein-Uhlenbeck process with time-variable infinitesimal mean (drift) and variance. The Ornstein-Uhlenbeck process is probably the most common neuronal model of this type, and the variability of its infinitesimal moments reflects that of the input signal, which is represented by the electric current. Furthermore, in this study, the firing part of the model is not considered, and the model is studied in the absence of spike generation. The existence of firing would not change the results but would make the method notationally complicated. We selected the Ornstein-Uhlenbeck neuronal model because it permits us to infer the role of the parameters and functions appearing in the model and their ranges. Otherwise, the quantities could be selected ad hoc and could be investigated in ranges completely outside any biological relevance.

A neuron receives synaptic inputs from many different excitatory and inhibitory presynaptic neurons. Under the leaky integration scenario and in the absence of firing, its membrane potential, $X = X(t)$, is described by a differential equation (Tuckwell, 1988),

$$\frac{dX}{dt} = -\frac{X(t) - x_L}{\tau} + I_{\mathrm{Exc}}(t) - I_{\mathrm{Inh}}(t); \qquad X(0) = x_L, \tag{2.1}$$

where

$$I_{\mathrm{Exc}}(t) = \sum_{i=1}^{N_E} a_E \sum_k \delta(t - t_{E,i}^k), \qquad I_{\mathrm{Inh}}(t) = \sum_{i=1}^{N_I} a_I \sum_k \delta(t - t_{I,i}^k). \tag{2.2}$$

x_L is the resting potential, $\tau > 0$ is the membrane time constant, and I_{Exc}, I_{Inh} represent contributions to the membrane potential due to the synaptic input from excitatory and inhibitory presynaptic neurons. The constants N_E (N_I) denote the number of excitatory (inhibitory) presynaptic neurons, $a_E > 0$ ($a_I > 0$) can be seen as the amplitudes of the excitatory (inhibitory) postsynaptic potentials, $t^k_{E,i}$ ($t^k_{I,i}$) is the kth spike time from the ith excitatory (inhibitory) presynaptic neuron, and $\delta(t)$ is a Dirac delta function.

In reality, we have no information about the exact timing of the input spike trains because they often appear as random with different rates. Therefore, it is often assumed that each excitatory and inhibitory presynaptic neuron produces its spike trains in accordance with a Poisson process with individual intensities $\lambda_{E,i}(t)$ ($i = 1, 2, \ldots, N_E$) and $\lambda_{I,i}(t)$ ($i = 1, 2, \ldots, N_I$). The model with the Poisson assumption is mathematically equivalent to the stochastic Stein's model (Stein, 1965; Tuckwell, 1988),

$$d X_t = -\frac{X_t - x_L}{\tau} dt + a_{\mathrm{E}} d P_t^+ - a_{\mathrm{I}} d P_t^-; \;\; X_0 = x_L, \tag{2.3}$$

where X_t is the membrane potential at time t and P_t^+, P_t^- are two independent nonhomogeneous Poisson processes with intensities $\lambda_E(t) = \sum_{i=1}^{N_E} \lambda_{E,i}(t)$ and $\lambda_I(t) = \sum_{i=1}^{N_I} \lambda_{I,i}(t)$, respectively. The first and the second infinitesimal moments of X defined by equation 2.3 are

$$M_1(x,t) = \lim_{\Delta t \to 0} \frac{E[\Delta X_t | X_t = x]}{\Delta t} = -\frac{x - x_L}{\tau} + a_{\mathrm{E}} \lambda_{\mathrm{E}}(t) - a_{\mathrm{I}} \lambda_{\mathrm{I}}(t), \tag{2.4}$$

$$M_2(x,t) = \lim_{\Delta t \to 0} \frac{E[(\Delta X_t)^2 | X_t = x]}{\Delta t} = a_{\mathrm{E}}^2 \lambda_{\mathrm{E}}(t) + a_{\mathrm{I}}^2 \lambda_{\mathrm{I}}(t), \tag{2.5}$$

where $\Delta X_t = X_{t+\Delta t} - X_t$ (Ricciardi, 1977).

In a general diffusion model, the membrane potential is described by a scalar diffusion process $V = V_t$ given by the Itô-type stochastic differential equation (Ricciardi, 1977),

$$d V_t = \nu(V_t; t) dt + \sigma(V_t; t) d W_t; \;\; V_0 = v_0, \tag{2.6}$$

where ν and σ are real-valued functions (called) respectively, a drift and an infinitesimal variance) of their arguments and W_t is a standard Wiener process (Brownian motion).

The first two infinitesimal moments of process 2.6 are $M_1(v,t) = \nu(v;t)$ and $M_2(v,t) = \sigma^2(v;t)$. Comparing the infinitesimal moments 2.4 and 2.5 of Stein's model with those of the general diffusion model, we can see that the diffusion approximation (Ricciardi, 1976; Lansky, 1984; Tuckwell, 1988)

of Stein's model is

$$dV_t = \left(-\frac{V_t - v_L}{\tau} + \mu(t)\right) dt + \sigma(t)\, dW_t; \qquad V_0 = v_L, \tag{2.7}$$

where

$$\mu(t) = a_{\mathrm{E}}\lambda_{\mathrm{E}}(t) - a_{\mathrm{I}}\lambda_{\mathrm{I}}(t), \tag{2.8}$$

$$\sigma^2(t) = a_{\mathrm{E}}^2\lambda_{\mathrm{E}}(t) + a_I^2\lambda_{\mathrm{I}}(t), \tag{2.9}$$

and $v_L = x_L$. Equation 2.9 shows the relation of the infinitesimal variance in diffusion neuronal model 2.7 to the drift 2.8. Despite the fact that in many applications, the variance $\sigma^2(t)$ in equation 2.7 is denoted as the amplitude of the noise, in neuronal context, due to equation 2.9, it is related to the signal (for more details, see Lansky & Sacerdote, 2001).

There are two kinds of quantities appearing in equations 2.1 to 2.3 and, consequently, also in equations 2.7 to 2.9. The first kind is the input signal $\mu(t)$ and $\sigma^2(t)$. For convenience, we call $\mu(t)$ a mean input signal and $\sigma^2(t)$ a variance input signal or variance. The activity of the neurons impinging on the studied one are characterized by the input rate $\lambda_E(t)$ and $\lambda_I(t)$. Therefore, under the rate coding principle, both $\mu(t)$ and $\sigma^2(t)$ in equation 2.7 are the input signal that we aim to determine. Under some specific conditions, the dependence between $\mu(t)$ and $\sigma^2(t)$ may cause counterintuitive situations; for example, if $a_E = a_I$ and $\lambda_E(t)$ and $\lambda_I(t)$ are periodic, completely synchronized, and balanced, then $\mu(t)$ is constant. Shifting the relative phases may result in constant $\sigma^2(t)$. In any case, equations 2.8 and 2.9 permit us to find the input intensities $\lambda_E(t)$ and $\lambda_I(t)$ if $\mu(t)$ and $\sigma^2(t)$ are known.

The second group of quantities in equation 2.7 is the intrinsic parameters of a neuron, such as the amplitudes of excitatory and inhibitory postsynaptic potentials a_E and a_I, the resting potential v_L and the membrane time constant τ. Although they may vary, they are relatively stable compared to the input signal. In addition, these parameters are measurable by means of additional experiments such as a voltage clamp technique.

3 Method

Our goal is to estimate the time-varying input signal $\{\mu(t), \sigma^2(t)\}_{t=0}^T$ from the observed voltage trace $\{V(t)\}_{t=0}^T$ given by equation 2.7, where $(0, T)$ is the observation interval. For that purpose, we assume that the resting potential v_L and the membrane time constants τ are known. Because the estimation problem is ill posed, we cannot determine the input signal from a voltage trace without additional assumptions. To overcome this, we employ a Bayesian approach and introduce random-walk-type priors

for the input signal. Then we determine hyperparameters by using the expectation-maximization (EM) algorithm. Finally, we evaluate the Bayesian estimate of the input signal with the Kalman filtering and smoothing techniques. Figure 1 gives a schematic description of the proposed method.

3.1 Prior Distribution of Input Signal. Let us assume that the voltage is sampled at N equidistant steps $t_j = jh,\ j = 1, \ldots, N$, where $h > 0$ is sampling step and the recorded voltage is denoted by $\{V_i\}$. Although there is no conceptual difference between considering equidistant steps and nonequidistant steps, we studied the equidistant case for simplicity. To apply the Bayesian approach, model 2.7 is modified into the discretized form

$$V_{j+1} = V_j + \left(-\frac{V_j - v_L}{\tau} + M_j\right)h + \sqrt{S_j h}\eta_j, \qquad V_0 = v_L, \tag{3.1}$$

where η_j are independent gaussian random variables of zero mean and unit standard deviation, and $\{M_j,\ S_j\}$ are sufficiently smooth random functions satisfying the following conditions (Bialek, Callan, & Strong, 1996; Kitagawa, 1998; Koyama & Shinomoto, 2005; Shimokawa & Shinomoto, 2009):

$$P[M_{j+1}|M_j = m] = N(m, \gamma_M^2 h), \tag{3.2}$$

$$P[S_{j+1}|S_j = s] = N(s, \gamma_S^2 h), \tag{3.3}$$

where γ_M^2 and γ_S^2 are the hyperparameters that regulate the smoothness of $\{M_j,\ S_j\}$ and $N(a, b)$ is the gaussian distribution with mean a and variance b.

Neuron model 3.1 and the prior distribution for input signal, equations 3.2 and 3.3, can be represented as the state-space model, in which $\vec{X}_j \equiv (M_j, S_j)$ are the two-dimensional (2D) states and $Z_j = V_{j+1} - V_j + \frac{V_j - v_L}{\tau}h \ \ (j = 1, \ldots, N-1)$ are the observations. The state equation derived from equations 3.2 and 3.3 is

$$\vec{X}_{j+1} = F\vec{X}_j + \vec{\xi}_j, \tag{3.4}$$

where F is the state transition matrix and $\vec{\xi}_j$ is the process noise drawn from a zero mean 2D gaussian distribution with covariance G, that is, $\vec{\xi}_j \sim N(\vec{0}, G)$. F and G are 2×2 diagonal matrices and given by

$$F = \mathrm{diag}(1, 1), \quad G = \mathrm{diag}(\gamma_M^2 h, \gamma_S^2 h).$$

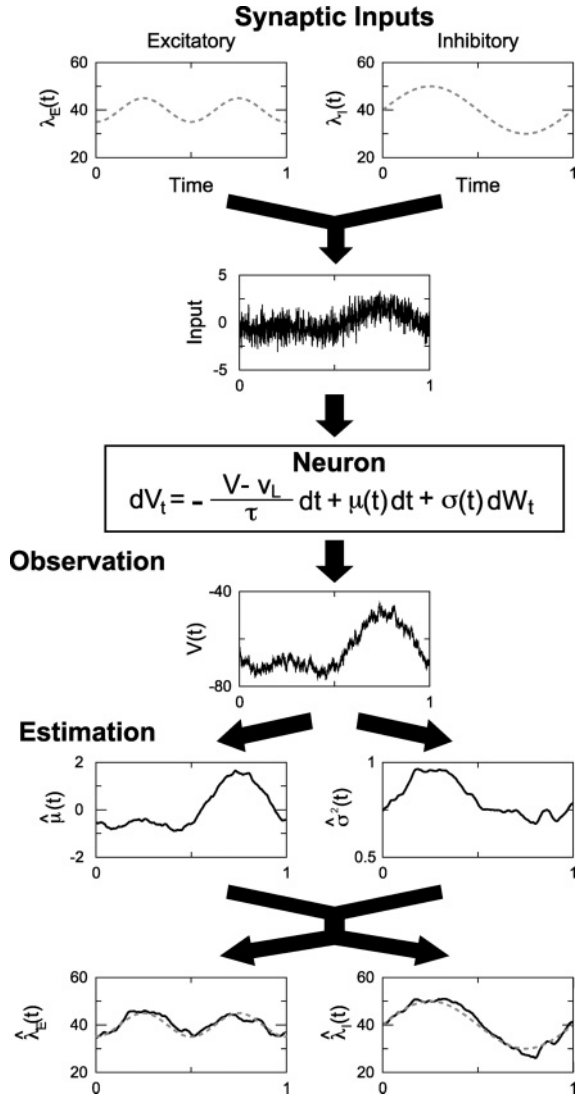

Figure 1: Schematic representation of the estimation procedure (for details, see the text). A neuron is driven by a large number of time-variable synaptic inputs from excitatory and inhibitory neurons. The second panel shows the total input to a neuron. The formal description of the neuron is given by the equation below. The membrane voltage, shown in the fourth panel from top, is observed. The mean input signal and the variance input signal are estimated from the voltage trace with a Bayesian filter. Finally, the excitatory and inhibitory firing rates can be deduced.

The observation equation derived from equation 3.1 is

$$Z_j = M_j h + \sqrt{S_j h}\eta_j. \tag{3.5}$$

3.2 Posterior Distribution of Input Signal. To estimate the paths of input parameters for the given data, we first determine the smoothness of the mean and variance of input signal, which is characterized by $\theta := (\gamma_M^2, \gamma_S^2)$, by maximizing the likelihood via the EM algorithm (Dempster, Laird, & Rubin, 1977). The likelihood integrated over hidden variables $\{\vec{X}_j\}_{j=1}^{N-1}$ is maximized,

$$\vec{\theta}_{\mathrm{ML}} = \underset{\vec{\theta}}{\operatorname{argmax}}\, p(Z_{1:N-1}|\vec{\theta}) = \underset{\vec{\theta}}{\operatorname{argmax}} \int p(Z_{1:N-1}, \vec{X}_{1:N-1}|\vec{\theta})\, d\vec{X}_{1:N-1}, \tag{3.6}$$

where $Z_{1:N-1} := \{Z_j\}_{j=1}^{N-1}$, $\vec{X}_{1:N-1} := \{\vec{X}_j\}_{j=1}^{N-1}$, and $d\vec{X}_{1:N-1} := \Pi_{j=1}^{N-1} d\vec{X}_j$. The maximization can be achieved iteratively by maximizing the Q function, the conditional expectation of the log likelihood

$$\theta_{k+1} = \underset{\theta}{\operatorname{argmax}}\, Q(\theta|\theta_k), \tag{3.7}$$

where, $Q(\theta|\theta_k) := E[\log(P[Z_{1:N-1}; \vec{X}_{1:N-1}|\theta])|Z_{1:N-1}, \theta_k]$ and θ_k is the kth iterated estimate of θ. The Q function can be written as

$$\begin{aligned} Q(\theta|\theta_k) = &\sum_{j=1}^{N-1} E[\log(P[Z_j|\vec{X}_j])\,|Z_{1:N-1}, \theta_k] \\ &+ \sum_{j=1}^{N-2} E[\log(P[\vec{X}_{j+1}|\vec{X}_j, \theta])\,|Z_{1:N-1}, \theta_k] + const. \end{aligned} \tag{3.8}$$

The $(k+1)$th iterated estimate of θ is determined by the conditions for

$$\frac{\partial Q}{\partial \gamma_M^2} = 0, \quad \frac{\partial Q}{\partial \gamma_S^2} = 0:$$

$$\gamma_{M,k+1}^2 = \frac{1}{(N-2)h} \sum_{j=1}^{N-2} E[(M_{j+1} - M_j)^2|Z_{1:N-1}, \theta_k], \tag{3.9}$$

$$\gamma_{S,k+1}^2 = \frac{1}{(N-2)h} \sum_{j=1}^{N-2} E[(S_{j+1} - S_j)^2|Z_{1:N-1}, \theta_k], \tag{3.10}$$

where $\gamma^2_{M,k}$, $\gamma^2_{S,k}$ are the kth iterated estimates of γ^2_M, γ^2_S, respectively. As the EM algorithm increases the marginal likelihood at each iteration, the estimate converges to a local maximum. We calculate the conditional expectations in equations 3.9 and 3.10 using Kalman filtering and smoothing algorithm (Kitagawa, 1998; Smith & Brown, 2003; Eden et al., 2004; Koyama & Shinomoto, 2005; Shimokawa & Shinomoto, 2009; Koyama, Perez-Bolde, Shalizi, & Kass, 2010; Paninski et al., 2010; see appendix A).

After fitting the hyperparameters, the Bayesian estimator for the input signal $\{\hat{\mu}_j, \hat{\sigma}^2_j\}_{j=1}^N$ is obtained from

$$\hat{\mu}_j = E[M_j | Z_{1:N-1},\ \gamma^2_M,\ \gamma^2_S], \tag{3.11}$$

$$\hat{\sigma}^2_j = E[S_j | Z_{1:N-1},\ \gamma^2_M,\ \gamma^2_S]. \tag{3.12}$$

We evaluate the estimator equations 3.11 and 3.12, using Kalman filtering and the smoothing algorithm. We determined, the excitatory and inhibitory input intensities from equations 2.8 and 2.9. We do not pursue the task up to this point as an additional assumption; knowlege of a_E and a_I, has to be postulated.

4 Applications

This section illustrates the efficiency of the method we have proposed. Recording the membrane voltage of a neuron *in vivo* is a tractable task with the current technology. However, the time course of the full input signal to the neuron is not available. Thus, we checked the proposed method by using simulated data. The voltage traces were generated from the Ornstein-Uhlenbeck model, equation 2.7. The parameters of the neuron were fixed at $v_L = -65$ mV and $\tau = 10$ ms. The simulation time step was fixed at $dt = 0.01$ ms. The voltage trace was sampled with the sampling step $h = 0.1$ ms, and the observation length was $T = 1$s except in sections 4.3 and 4.4. Using the EM algorithm described in the previous section, we determined the hyperparameters, γ^2_M and γ^2_S. The convergence criterion for the algorithm was that relative changes in the parameter iterations were to be lower than 10^{-4}, that is, $|new - old|/|old| < 10^{-4}$.

The estimation precision of the input signal $\mu(t), \sigma^2(t)$ was analyzed. To evaluate the precision, we calculated the integrated squared error (ISE) between the true input signal $s(t)$ and its estimate $\hat{s}(t)$,

$$R_s = \sqrt{\frac{1}{T}\int_0^T (\hat{s}(t) - s(t))^2 dt}, \tag{4.1}$$

The mean and the standard deviation of the ISE were evaluated from 100 realizations of simulated voltage traces.

We studied two types of time-varying input signals, continuous and discontinuous input. The range of the input signals μ, σ^2 was determined from experimental studies. The recorded membrane potential varied between -80 mV and -50 mV, and the standard deviation of the membrane potential was between 1 mV and 6 mV (Pare, Shink, Gaudreau, Destexhe, & Lang, 1998; Destexhe, Rudolph, & Pare, 2003). Here, we chose $-2 < \mu < 2, 0 < \sigma^2 < 4$. This implies that the asymptotic moments of model 2.7, that is, the mean and the standard deviation, are $-85 \le E[V_\infty] \le -45$, $0 \le \sqrt{\mathrm{Var}[V_\infty]} \le 4.5$.

4.1 Estimating Modulated Continuous Input. The test input signal $\mu(t)$, $\sigma^2(t)$ was sinusoidally modulated. We adopted

$$\mu(t) = C_\mu + A_\mu \sin(2\pi f_\mu t),\ \sigma^2(t) = C_{\sigma^2} + A_{\sigma^2} \sin(2\pi f_{\sigma^2} t), \tag{4.2}$$

where C_μ and C_{σ^2} were the constant levels of the input, A_μ and A_{σ^2} were the amplitudes, and f_μ and f_{σ^2} were the frequencies. The input signals were modulated at from 1 Hz to 10 Hz. Four types of the input signals are illustrated in Figure 2. We investigated the estimation precision for three types of input: constant signal (see Figure 2A), mean modulated signal (see Figure 2B), and variance modulated signal (see Figure 2C).

We examined the influence of variability of the input signal on the accuracy of the estimates. Figure 3 shows the ISE R_μ, R_{σ^2} as a function of the amplitude A_μ, A_{σ^2} (see Figure 3B), the frequency f_μ, f_{σ^2} (see Figure 3C), and the constant level C_μ, C_{σ^2} (see Figure 3D). We can see from Figure 3B that as the amplitude of an input signal grows, the ISE of the time-varying signal increases. The ISE of the other constant input signal, however, does not depend on the amplitude. We can see from Figure 3C that as the frequency of an input signal grows, the ISE of the time-varying signal increases. The ISE of the other constant input signal does not depend on the frequency. The dependence of frequency is similar to that of the amplitude. We can see from Figure 3D that as the constant level of input variance grows, the ISE of both input signals increases. On the contrary, as the constant level of input mean grows, the ISE of these input signals does not increase.

4.2 Estimating Constant Input with a Jump. We examined the effect of discontinuity in the input signal on the estimate precision. The input signal was taken in the form,

$$s(t) = s_0 + \delta s H\left(t - \frac{T}{2}\right), \tag{4.3}$$

where $s(t)$ represents $\mu(t)$ or $\sigma^2(t)$, s_0 is the initial value, δs is the jump size, and T is the observation length. $H(t)$ is the unit step function:

$$H(t) = \begin{cases} 0 & (x < 0) \\ 1 & (x \ge 0) \end{cases}.$$

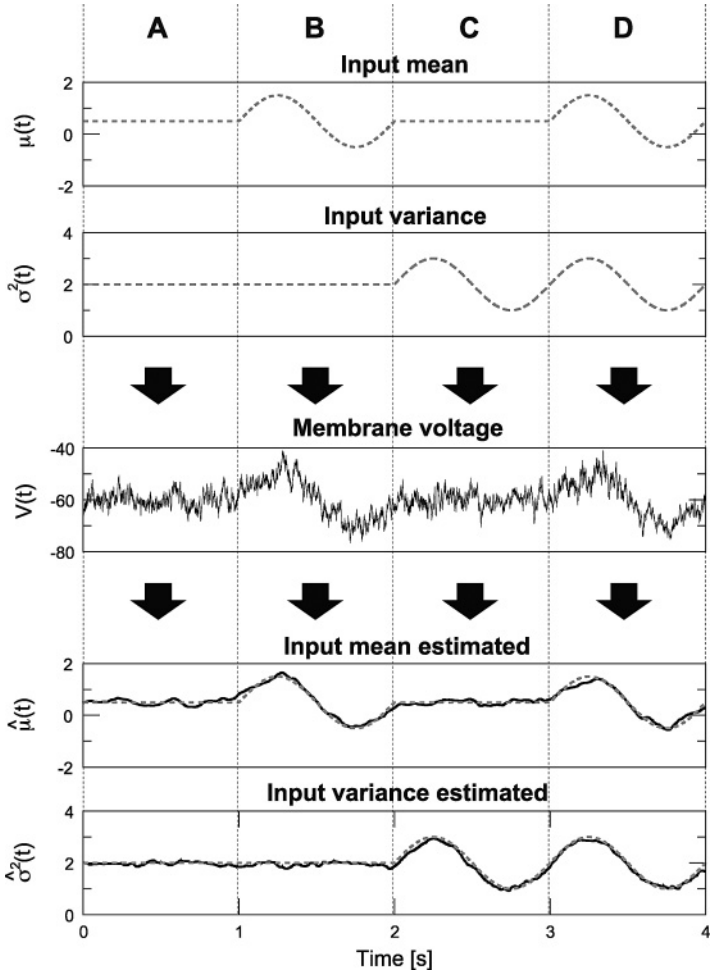

Figure 2: An example of four types of time-varying input signals and its estimates. (A) Both input signals are constant: $\mu(t) = 0.5$, $\sigma^2(t) = 2$. (B) The mean input is modulated, and the variance is constant: $\mu(t) = 0.5 + \sin(2\pi t)$, $\sigma^2(t) = 2$. (C) The mean input is constant, and the variance is modulated: $\mu(t) = 0.5$, $\sigma^2(t) = 2 + \sin(2\pi t)$. (D) Both input signals are modulated: $\mu(t) = 0.5 + \sin(2\pi t)$, $\sigma^2(t) = 2 + \sin(2\pi t)$.

First, we examined how the jump size of the input signal influences the accuracy of the estimates. Figure 4 shows the ISE R_μ, R_{σ^2} as a function of the jump size $\delta\mu$, $\delta\sigma^2$. We can see from Figure 4B that as the jump size of an input signal grows, the ISE of the time-varying signal increases. The ISE of the other constant input signal is independent of the jump size. Second, we

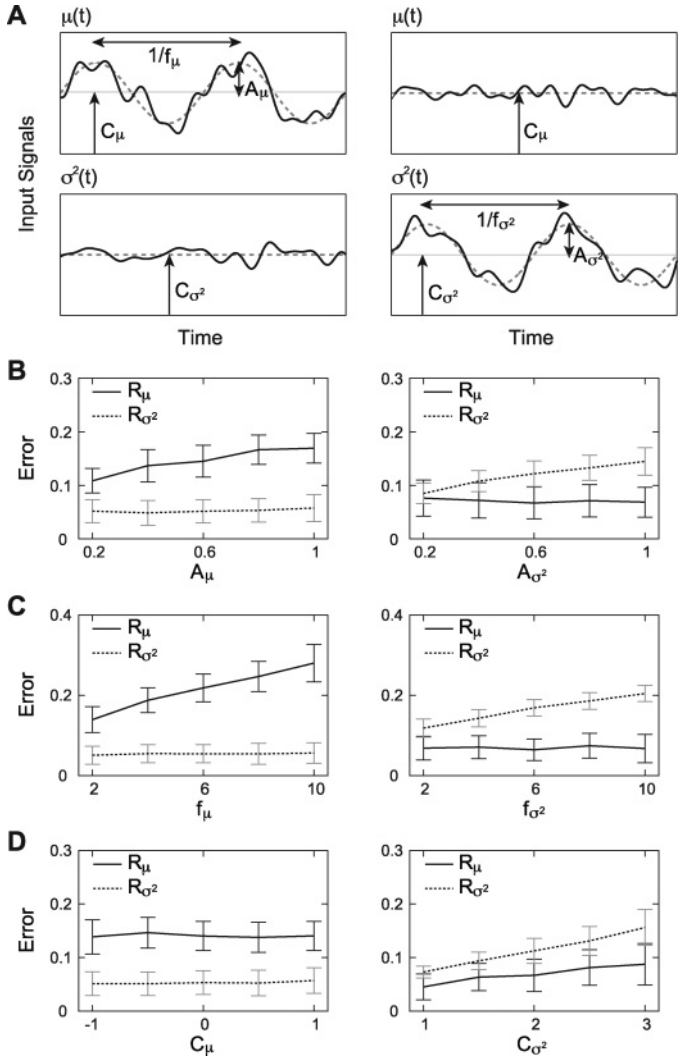

Figure 3: Dependence of the errors on the properties of sinusoidal input. (A) Schematic figures of the analysis of the estimation errors. (B–D). The dependence of the errors (R_μ, R_{σ^2}) and their standard deviation on the amplitude A_μ, A_{σ^2} (B), the frequency f_μ, f_{σ^2} (C), and the base line C_μ, C_{σ^2} (D) are shown. The black lines represent the mean of R_μ, and the dotted lines represent that of R_{σ^2}. The black error bars are the the standard deviation of R_μ, and the gray error bars are that of R_{σ^2}. The parameters in B are $f_\mu = 2$ (left figure), $f_{\sigma^2} = 2$ (right figure), $C_\mu = 0$, and $C_{\sigma^2} = 2$. Those in C are $A_\mu = 0.5$ (left), $A_{\sigma^2} = 0.5$ (right), $C_\mu = 0$, and $C_{\sigma^2} = 2$. Those in D are $A_\mu = 0.5$, $f_\mu = 2$, and $C_{\sigma^2} = 2$ (left), $A_{\sigma^2} = 0.5$, $f_{\sigma^2} = 2$ and $C_\mu = 0$ (right).

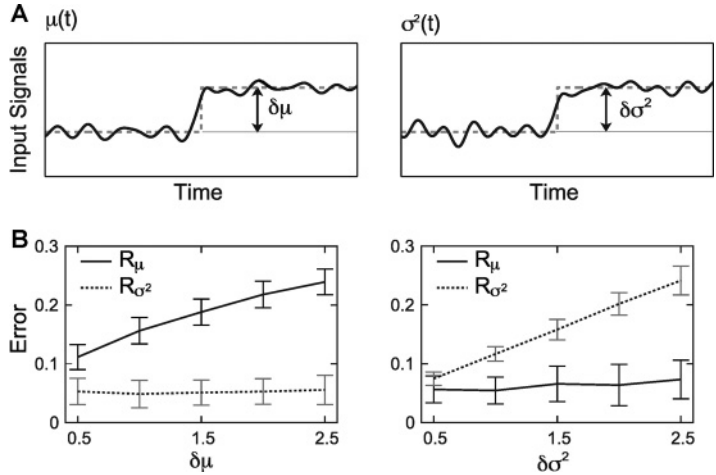

Figure 4: Dependence of errors on the properties of constant input with a jump. (A) Schematic figures of the analysis of the estimation errors. (B) The dependence of errors (R_μ, R_{σ^2}) and their standard deviation on the jump size $\delta\mu$, $\delta\sigma^2$ are shown. The black lines represent the mean of R_μ, and the dotted lines represent that of R_{σ^2}. The black error bars are the standard deviation of R_μ, and the gray error bars are that of R_{σ^2}. The parameters in B are $\mu_0 = -1, \sigma_0^2 = 2$ (left) and $\mu_0 = 0, \sigma_0^2 = 1$ (right).

examined the error dependence on the initial value of the input signal μ_0 and σ_0^2 (data not shown). The ISEs R_μ, R_{σ^2} do not depend on μ_0 but increase as a function of σ_0^2, as in the sinusoidal input signals (see Figure 3D).

4.3 The Effect of Sampling and Length of Data. We examined the effect of observation parameters such as the sampling interval and the observation duration on the accuracy of the estimates. For the constant input signals, the estimation error of the proposed method was compared with that of the maximum likelihood method (Lansky & Ditlevsen, 2008). For constant input signals, $\mu(t) = \mu$, $\sigma^2(t) = \sigma^2$, the maximum likelihood estimates can be given by

$$\hat{\mu}_{\mathrm{ML}} = \frac{1}{(N-1)h} \sum_{j=1}^{N-1} (V_{j+1} - AV_j), \tag{4.4}$$

$$\hat{\sigma}^2_{\mathrm{ML}} = \frac{1}{(N-1)h} \sum_{j=1}^{N-1} (V_{j+1} - AV_j - \hat{\mu}_{\mathrm{ML}} h)^2, \tag{4.5}$$

where $A = 1 - \frac{h}{\tau}$.

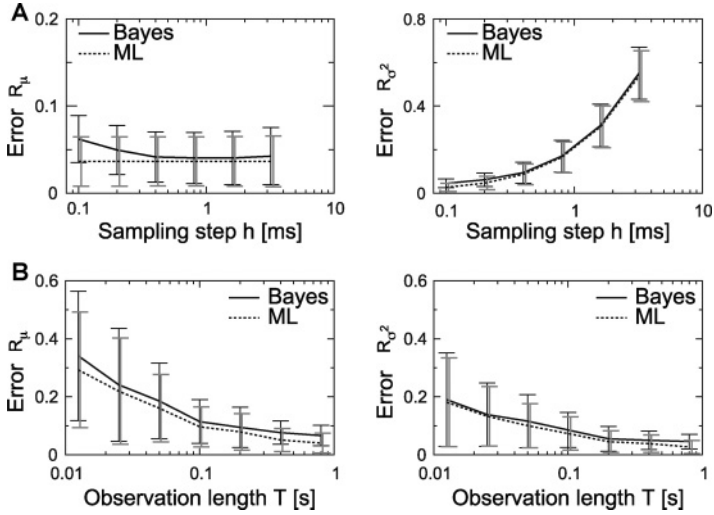

Figure 5: Dependence of errors on the observation parameters. (A) Dependence of errors (R_μ, R_{σ^2}) on the sampling step h. (B) Dependence of errors on the observation length T. The black lines represent the mean error of the Bayesian (Bayes) method, and the dotted lines represent that of maximum likelihood (ML) method. The black error bars are the standard deviation of the errors of the Bayes method, and the gray error bars are that of ML method. The same constant input signals are examined: $C_\mu = 0$ and $C_{\sigma^2} = 2$.

Figure 5 shows the dependence of the ISE R_μ, R_{σ^2} of the constant signals on the sampling step h (see Figure 5A) and the observation length T (see Figure 5B). We can see from Figure 5A that as the sampling step grows, the ISEs of the input variance increases, while that of the input mean does not increase. Both ISEs decrease as a function of the observation length, as shown in Figure 5B. These results document that the estimate precision of the proposed method is as good as that of the maximum likelihood method for constant input signals.

4.4 Realistic Model. The results obtained above are for a simplified model with synaptic input. It is assumed that the synaptic input is additive (current) and the time course of each input is a Dirac delta function. It may evoke a question of what the performance of the method would be if applied to more realistic models and consequently, the experimental data. To get insight into this problem, we applied the proposed method to a more realistic model of a neuron *in vivo* (Destexhe, Mainen, & Sejnowski, 1998; Rudolph, Piwkowska, Badoual, Bal, & Destexhe, 2004), which captures two realistic features of the synaptic input: (1) the synaptic inputs are conductance (state dependent) input, and (2) each synaptic input consists

of a sharp rise followed by an exponential decay. The details of the model are summarized in the appendix B. This model was simulated, but the estimation procedure was based on leaky integrator with input currents (see equation 2.7.

We estimated the mean and variance of the input current $\{\mu(t), \sigma^2(t)\}$, and the input rates $\{\lambda_E(t), \lambda_I(t)\}$ are estimated using equations 2.8 and 2.9. We considered the situation that the excitatory input rate was modulated and the inhibitory one was constant. As in the previous sections, we simulated sinusoidally modulated input (see equation 4.2) and constant input with a jump (see equation 4.3),

$$\lambda_{E,i}(t) = E_0 + E_1 \sin(\omega t), \quad \lambda_{I,i}(t) = I_0, \tag{4.6}$$

$$\lambda_{E,i}(t) = E_0 + \delta E \; H\left(t - \frac{T}{2}\right), \quad \lambda_{I,i}(t) = I_0, \tag{4.7}$$

where $\lambda_{E(I),i}(t)$ is the firing rate of each excitatory (inhibitory) presynaptic neuron and $H(t)$ is the unit step function. An example of results is shown in Figure 6. We can expect that there will be an error when using the method because the simulated data do not satisfy the assumptions that the synaptic inputs are additive and a Dirac delta function. Although there are deviations between the true inputs and their estimates, these deviations are small. This method still provides an accurate estimate of the synaptic input for the more realistic model.

5 Discussion

Several methods for estimating input signal from the voltage data have been proposed up to now. The first is based on the maximum likelihood principle. In Lansky (1983), the maximum likelihood estimator for constant input signal in the Ornstein-Uhlenbeck model was developed. The method was applied to the experimental data in Lansky, Sanda, and He (2006, 2010). In Pospischil, Piwkowska, Bal, & Destexhe (2009), the maximum likelihood method for estimating the constant excitatory and inhibitory synaptic conductances is also developed and applied to the experimental data. The second method is based on the method of moments. Lansky et al. (2006, 2010) fit the mean and standard deviation of the Ornstein-Uhlenbeck process to the data and compared the results obtained by this method with those from the maximum likelihood method. These two methods are applicable to the single-trial voltage data if the constancy of input signal can be assumed. The third method is based on the approximate formula for the steady-state membrane potential distribution. Such a formula was derived in Rudolph and Destexhe (2003, 2005) and Lindner and Longtin (2006), and the constant excitatory and inhibitory input conductances were estimated

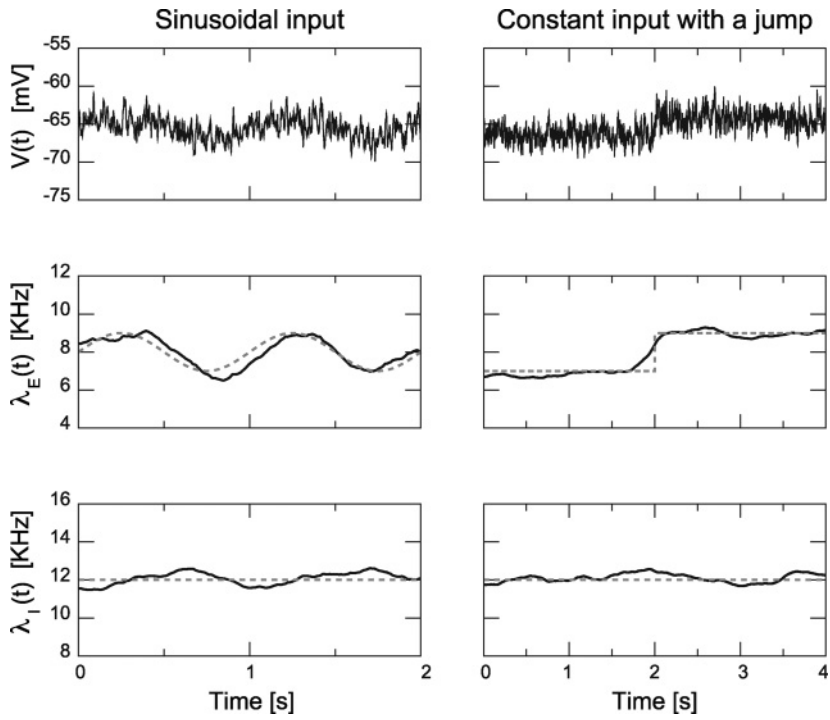

Figure 6: Estimation of synaptic inputs from membrane potential generated by a realistic synaptic model (for details, see appendix B). (A) Voltage traces used for the estimation. Input parameters are $E_0 = 8.0$ Hz, $E_1 = 1.0$ Hz, $\omega = 2\pi$ rad/s, and $I_0 = 12$ Hz (Left); $E_0 = 7.0$ Hz, $\delta E = 2.0$ Hz, and $I_0 = 12$ Hz (right). (B) Estimates of total input excitatory firing rate $\lambda_E(t)$. (C) Estimates of total input inhibitory firing rate $\lambda_I(t)$. The dashed lines are the true input rates and the solid black lines are their estimates. Parameters used for the estimation are $a_E = 0.08$ mV, $a_I = 0.1$ mV, $V_L = -60$ mV, and $h = 1.0$ ms (left); $a_E = 0.1$ mV, $a_I = 0.08$ mV, $V_L = -63$ mV, and $h = 1.0$ ms (right).

by fitting the model to the observed voltage distribution of Rudolph et al. (2004) and Rudolph, Pospischil, Timofeev, & Destexhe (2007). This method is also based on the assumption of constancy of the input signals, and it requires at least two voltage traces whose means are different. The fourth method is based on the repetition of experimental trials. This method succeeded in estimating time-varying synaptic inputs from *in vivo* and *in vitro* data (Borg-Graham, Monier, & Frégnac, 1998; Wehr & Zador, 2003; Monier, Fournier, & Frégnac, 2008). The disadvantage of this method is the requirement of a high number of replicated trials with identical input signals. Thus,

at least at this moment, this method is applicable only to sensory neurons where the signal can be precisely controlled.

Contrary to these methods, our proposed technique requires neither the constancy of the input nor the repetition of experimental trials. It is based on four fundamental assumptions. First, the fluctuations of the membrane potential can be closely described by the leaky integrator model. This is not a very restrictive assumption since it has been shown that the Hodgkin-Huxley models can be approximated by leaky integrate-and-fire models quite accurately (Kistler et al., 1997; Jolivet et al., 2004; Kobayashi & Shinomoto, 2007). Second, the proposed method is based on a simplified model of the synaptic input. This is a current input model, which means that the input is state (voltage) independent. This was also considered in previous studies (Softky & Koch, 1993; Shadlen & Newsome, 1995, 1998; Pham, Pakdaman, & Vibert, 1998; Diesmann, Gewaltig, & Aertsen, 1999; Shinomoto, Sakai, & Funahashi, 1999; DeWeese & Zador, 2006; Lansky et al., 2006, 2010; Jolivet et al., 2008; Kobayashi, Tsubo, & Shinomoto, 2009; Vilela & Lindner, 2009). In realistic models, the synaptic input is described as a conductance input, which means that the input is state (voltage) dependent. In addition, Stein's model assumed that a single synaptic input is described as a Dirac delta function, which causes a discontinuous jump of the membrane potential. However, the time course of the synaptic input in real neurons consists of a sharp rise followed by an exponential decay. We also assumed the homogeneity (fixed amplitude) of the synaptic input. As shown in numerical examples (see Figure 6), some of these assumptions are not restrictive, and the method seems to be robust against their violation. The results indicate that the estimated infinitesimal mean and variance of the model $\{M_j, S_j\}$ reflect the excitatory and inhibitory input rates in the biophysical realistic model (see appendix B). The estimated moments also reflect the mean and variance of the synaptic conductances estimated in previous work (Rudolph et al., 2004, 2007; Pospischil et al., 2009). Third, the voltage is recorded without observation noise. It is true that in the voltage-sensitive imaging, the voltage is contaminated with high observation noise (Huys & Paninski, 2009). On the other hand, when intracellular recordings are used, the voltage is available practically noise free. Furthermore, a sophisticated method for high-resolution intracellular recordings was presented in Brette et al. (2008). Therefore, this assumption is reasonable for the intracellular data. Fourth, the intrinsic neural parameters, such as the resting potential and the membrane time constant, have to be known in advance. However, it should be noted that the proposed method can be extended to include the estimation of these parameters. Similarly, the method can also be extended for realistic neuronal models but it is beyond the scope of this letter.

Potential application of the proposed technique would be to estimate time-variable excitatory and inhibitory synaptic input rates from *in vivo* recorded membrane potential (Borg-Graham et al., 1998; Wehr & Zador,

2003; DeWeese and Zador, 2006; Monier et al., 2008). In general, it can be applied to the experimental data in the present form under the condition that the Ornstein-Uhlenbeck model describes them sufficiently well. It is shown that some of the voltage traces recorded *in vivo* can be well described by this model (DeWeese & Zador, 2006; Lansky et al., 2006, 2010). However, in actual neurons, the synaptic input causes a change in conductance, and the time course of each input is exponential. The difference between the current input model and actual neurons is prominent if the voltage trace fluctuates largely. The Ornstein-Uhlenbeck model might not describe that kind of voltage traces well. In that case, extensions of our framework to the realistic model would be useful for such situations. Such extensions would allow us to estimate biophysical parameters (input conductances) from a voltage trace.

In this study, we presented a new method for estimating time-varying input signal from the membrane voltage of a neuron (see Figure 1). The proposed method provides accurate estimates of both continuous and discontinuous signals (see Figures 2–4). Though discontinuous signals do not satisfy an assumption of slow variability, the method is applicable for these signals. For a constant signal, the estimation performance of the method is comparable to that of the maximum likelihood method (see Figure 5). As illustrated with the simulated data, the method is efficient and precise. The price for its high flexibility and efficiency is a relatively high computational complexity. Nevertheless, all the results suggest that the new method may be useful for studying the input-output relationship in neurons.

Appendix A: Kalman Filtering and Smoothing Algorithm

We describe a procedure for calculating conditional expectations in equations 3.9 and 3.10 based on state equation 3.4 and observation equation 3.5.

For notational simplicity, we introduce $\vec{x}_{j|n}$, $\Sigma_{j|n}$ and $\Sigma_{i,j|n}$ defined by

$$\vec{x}_{j|n} := E[\vec{X}_j | Z_{1:n}], \tag{A.1}$$

$$\Sigma_{j|n} := E[(\vec{X}_j - \vec{x}_{j|n})(\vec{X}_j - \vec{x}_{j|n})^T | Z_{1:n}], \tag{A.2}$$

$$\Sigma_{i,j|n} := E[(\vec{X}_i - \vec{x}_{i|n})(\vec{X}_j - \vec{x}_{j|n})^T | Z_{1:n}]. \tag{A.3}$$

For evaluating equations 3.9 and 3.10, we need to calculate conditional expectations $\{\vec{x}_{j|N-1}\}_{j=1}^{N-1}$ and conditional covariances $\{\Sigma_{j+1,j|N-1}\}_{j=1}^{N-1}$ from the observation.

A.1 Prediction Algorithm. The mean and covariance of the predictive distribution $\vec{x}_{j+1|j}$, $\Sigma_{j+1|j}$ may be calculated from that of the filtered

distribution $\vec{x}_{j|j}$, $\Sigma_{j|j}$:

$$\vec{x}_{j+1|j} = F\vec{x}_{j|j}, \tag{A.4}$$

$$\Sigma_{j+1|j} = F\Sigma_{j|j}F^T + G. \tag{A.5}$$

A.2 Filtering Algorithm. Using the Bayes theorem, the filtered distribution may be written as

$$\begin{aligned} P[\vec{x}_j|Z_{1:j}] &= \frac{P[Z_j|\vec{x}_j,\ Z_{1:j-1}]P[\vec{x}_j|Z_{1:j-1}]}{P[Z_j]} \\ &\propto P[Z_j|\vec{x}_j]P[\vec{x}_j|Z_{1:j-1}]. \end{aligned} \tag{A.6}$$

The filtered distribution may be approximated to the gaussian distribution by Taylor-expanding its logarithm up to the second-order term (Laplace approximation; Smith & Brown, 2003; Eden et al., 2004; Koyama, Perez-Bolde, et al., 2010). The mean and covariance of the filtered distribution $\vec{x}_{j|j}$, $\Sigma_{j|j}$ can be given by

$$\frac{d}{d\vec{x}_j}\log p(\vec{x}_j|Z_{1:j})|_{\vec{x}_{j|j}} = 0, \tag{A.7}$$

$$\Sigma_{j|j}^{-1} = -H(\log p(\vec{x}_j|Z_{1:j}))|_{\vec{x}_{j|j}}, \tag{A.8}$$

where $H(f)$ is the Hessian matrix of f.

A.3 Smoothing Algorithm. The mean and covariance of the smoothed distribution $\vec{x}_{j|N-1}$, $\Sigma_{j|N-1}$ can be given by (Smith & Brown, 2003)

$$\vec{x}_{j|N-1} = \vec{x}_{j|j} + A_j(\vec{x}_{j+1|N-1} - \vec{x}_{j+1|j}), \tag{A.9}$$

$$\Sigma_{j|N-1} = \Sigma_{j|j} + A_j(\Sigma_{j+1|N-1} - \Sigma_{j+1|j})A_j^T, \tag{A.10}$$

where

$$A_j = \Sigma_{j|j}F\Sigma_{j+1|j}^{-1}. \tag{A.11}$$

A.4 Covariance Algorithm. The covariance algorithm for calculating the conditional covariance $\Sigma_{j+1,\,j|N-1}$ is given by

$$\Sigma_{j+1,\,j|N-1} = A_j\Sigma_{j+1|N-1}. \tag{A.12}$$

From these equations, we can evaluate the conditional variances in equations 3.9 and 3.10 using $\vec{x}_{j|N-1}$, $\Sigma_{j|N-1}$ and $\Sigma_{j+1,j|N-1}$,

$$E[(M_{j+1}-M_j)^2|Z_{1:N-1},\theta_k] = \left(x^{(1)}_{j+1|N-1}-x^{(1)}_{j|N-1}\right)^2+\Sigma^{(1,1)}_{j+1|N-1} +\Sigma^{(1,1)}_{j|N-1}-2\Sigma^{(1,1)}_{j+1,j|N-1}, \tag{A.13}$$

$$E[(S_{j+1}-S_j)^2|Z_{1:N-1},\theta_k] = \left(x^{(2)}_{j+1|N-1}-x^{(2)}_{j|N-1}\right)^2+\Sigma^{(2,2)}_{j+1|N-1} +\Sigma^{(2,2)}_{j|N-1}-2\Sigma^{(2,2)}_{j+1,j|N-1}, \tag{A.14}$$

where $x^{(k)}_{j|N-1}$ is the k component of the vector $\vec{x}_{j|N-1}$, $\Sigma^{(k,l)}_{j|N-1}$ is the (k,l) component of the matrix $\Sigma_{j|N-1}$ and $\Sigma^{(k,l)}_{j+1,j|N-1}$ is the (k,l) component of the matrix $\Sigma_{j+1,j|N-1}$.

Appendix B: A Single-Compartment Neuronal Model with Realistic Synaptic Inputs

Single-compartment neuronal model with realistic synaptic inputs (Destexhe et al., 1998; Rudolph et al., 2004) can be summarized in the following way. The membrane potential of a neuron $V(t)$ is described by

$$C_m\frac{dV}{dt} = -g_L(V-E_L)+\frac{1}{a}I_{\mathrm{Exc}}(t)+\frac{1}{a}I_{\mathrm{Inh}}(t), \tag{B.1}$$

where C_m is the membrane capacitance, g_L is the leak conductance density, E_L is the resting potential, and a is the membrane area. The membrane parameters are $C_m = 1\ \mu\mathrm{F/cm}^2$, $g_L = 0.0452\ \mathrm{mS/cm}^2$, $E_L = -80$ mV, and $a = 34{,}636\ \mu\mathrm{m}^2$. The synaptic currents are given by

$$I_{\mathrm{Exc}}(t) = -\sum_{k=1}^{N_E} g_{\mathrm{AMPA}}m^k_e(t)(V-E_e), \tag{B.2}$$

$$I_{\mathrm{Inh}}(t) = -\sum_{k=1}^{N_I} g_{\mathrm{GABA}}m^k_i(t)(V-E_i), \tag{B.3}$$

where $g_{\mathrm{AMPA(GABA)}}$ is the quantal conductance of an AMPA (GABA) receptor respectively, $E_{e(i)}$ is the reversal potential of excitatory (inhibitory) conductance, and $m^k_{e(i)}$ represents the fractions of postsynaptic receptors in the open state at each excitatory (inhibitory) synapse. The dynamics of $m^k_{e,i}$ are

given by kinetic equations,

$$\frac{dm_{e,i}}{dt} = \alpha_{e,i} T(t)(1 - m_{e,i}) - \beta_{e,i} m_{e,i}, \tag{B.4}$$

where $T(t)$ is the transmitter concentration in the cleft and $\alpha_{e(i)}$ and $\beta_{e(i)}$ are forward and backward binding rate constants for excitatory (inhibitory) synapse. When a spike occures in the presynaptic compartment, a transmitter pulse is triggered such that $T = T_{\max}$ for a short period t_{dur} and $T = 0$ until the next spike occurs. The synaptic parameters are $N_E = 1000$, $N_I = 1000$, $g_{\mathrm{AMPA}} = 1800$ pS, $E_e = 0$ mV, $\alpha_e = 1.1 \times 10^6\,\mathrm{M^{-1}s^{-1}}$, $\beta_e = 670\,\mathrm{s^{-1}}$ for AMPA receptors, $g_{\mathrm{GABA}} = 1200$ pS, $E_i = -75$ mV, $\alpha_i = 5.0 \times 10^6\,\mathrm{M^{-1}s^{-1}}$, $\beta_i = 180\,\mathrm{s^{-1}}$ for GABA receptors, $T_{\max} = 1$ mM, and $t_{\mathrm{dur}} = 1$ ms.

Acknowledgments

We are grateful to I. Nishikawa for helpful comments, and two anonymous referees for several comments that helped to improve the letter. R.K. is grateful for the kind hospitality of the Academy of Sciences of the Czech Republic. This study was supported by the Support Center for Advanced Telecommunications Technology Research Foundation, the Yazaki Memorial Foundation for Science and Technology, and Ritsumeikan University's Research Funding Research Promoting Program "Young Scientists (Start-up)", "General Research" to R.K., a Grant-in-Aid for Scientific Research from MEXT Japan (20300083) to S.S., and the Center for Neurosciences LC554, grant No. AV0Z50110509 and the Grant Agency of the Czech Republic, project P103/11/0282 to P.L.

References

Bialek, W., Callan, C. G., & Strong, S. P. (1996). Field theories for learning probability distributions. *Phys. Rev. Lett.*, *77*, 4693–4697.

Borg-Graham, L. J., Monier, C., & Frégnac, Y. (1998). Visual input evokes transient and strong shunting inhibition in visual cortical neurons. *Nature*, *393*, 369–373.

Brette, R., Piwkowska, Z., Monier, C., Rudolph-Lilith, M., Fournier, J., Levy, M., et al. (2008). High-resolution intracellular recordings using a real-time computational model of the electrode. *Neuron*, *59*, 379–391.

Burkitt, A. N. (2006). A review of the integrate-and-fire neuron model: I. Homogeneous synaptic input. *Biol. Cybern.*, *95*, 1–19.

Dempster, A. P., Laird, N. M., & Rubin, D. B. (1977). Maximum likelihood from incomplete data via the EM algorithm. *J. Roy. Stat. Soc. B*, *39*, 1–38.

Destexhe, A., Mainen, Z., & Sejnowski, T. J. (1998). Kinetic models of synaptic transmission. In C. Koch & I. Segev (Eds.), *Methods in neuronal modeling* (pp. 1–26). Cambridge, MA: MIT Press.

Destexhe, A., Rudolph, M., & Pare, D. (2003). The high-conductance state of neocortical neurons in vivo. *Nat. Rev. Neurosci.*, *4*, 739–751.

DeWeese, M. R., & Zador, A. M. (2006). Non-gaussian membrane potential dynamics imply sparse, synchronous activity in auditory cortex *J. Neurosci.*, *26*, 12206–12218.

Diesmann, M., Gewaltig, M. O., & Aertsen, A. (1999). Stable propagation of synchronous spiking in cortical neural networks. *Nature*, *402*, 529–533.

Eden, U. T., Frank, L. M., Barbieri, R., Solo, V., & Brown, E. N. (2004). Dynamic analyses of neural encoding by point process adaptive filtering. *Neural Comput.*, *16*, 971–998.

Friston, K. J., Penny, W., Phillips, C., Kiebel, S., Hinton, G., & Ashburner, J. (2002). Classical and Bayesian inference in neuroimaging: Theory. *NeuroImage*, *16*, 465–483.

Huys, Q.J.M., & Paninski, L. (2009). Smoothing of, and parameter estimation from, noisy biophysical recordings. *PLoS Comput. Biol.*, *5*, e1000379.

Jolivet, R., Kobayashi, R., Rauch, A., Naud, R., Shinomoto, S., & Gerstner, W. (2008). A benchmark test for a quantitative assessment of simple neuron models. *J. Neurosci. Methods*, *169*, 417–424.

Jolivet, R., Lewis, T. J., & Gerstner, W. (2004). Generalized integrate-and-fire models of neuronal activity approximate spike trains of a detailed model to a high degree of accuracy. *J. Neurophysiol.*, *92*, 959–976.

Kistler, W., Gerstner, W., & van Hemmen, J. L. (1997). Reduction of the Hodgkin-Huxley equations to a single-variable threshold model. *Neural Comput.*, *9*, 1015–1045.

Kitagawa, G. (1998). A self-organizing state-space model. *J. Am. Stat. Assoc.*, *93*, 1203–1215.

Kobayashi, R., & Shinomoto, S. (2007). State space method for predicting the spike times of a neuron. *Phys. Rev. E*, *75*, 011925.

Kobayashi, R., Tsubo, Y., & Shinomoto, S. (2009). Made-to-order spiking neuron model equipped with a multi-timescale adaptive threshold. *Front. Comput. Neurosci.*, *3*, 9.

Koyama, S., Chase, S. M., Whitford, A. S., Velliste, M., Schwartz, A. B., & Kass, R. E. (2010). Comparison of brain-computer interface decoding algorithms in open-loop and closed-loop control. *J. Comput. Neurosci.*, *29*, 73–87.

Koyama, S., Perez-Bolde, L. C., Shalizi, C. R., & Kass, R. E. (2010). Approximate methods for state-space models. *J. Am. Stat. Assoc.*, *105*, 170–180.

Koyama, S., & Shinomoto, S. (2005). Empirical Bayes interpretations of random point events. *J. Physics A*, *38*, L531–L537.

Lansky, P. (1983). Inference for the diffusion models of neuronal activity. *Math. Biosci.*, *67*, 247–260.

Lansky, P. (1984). On approximations of Stein's neuronal model. *J. Theor. Biol.*, *107*, 631–647.

Lansky, P., & Ditlevsen, S. (2008). A review of the methods for signal estimation in stochastic diffusion leaky integrate-and-fire neuronal models. *Biol. Cybern.*, *99*, 253–262.

Lansky, P., & Sacerdote, L. (2001). The Ornstein-Uhlenbeck neuronal model with signal-dependent noise. *Phys. Lett. A*, *285*, 132–140.

Lansky, P., Sanda, P., & He, J. (2006). The parameters of the stochastic leaky integrate-and-fire neuronal model. *J. Comput. Neurosci.*, *21*, 211–223.

Lansky, P., Sanda, P., & He, J. (2010). Effect of stimulation on the input parameters of stochastic leaky integrate-and-fire neuronal model. *J. Physiol. (Paris)*, *104*, 160–166.

Lindner, B., & Longtin, A. (2006). Comment on "Characterization of subthreshold voltage fluctuations in neuronal membranes," by M. Rudolph and A. Destexhe. *Neural Comp.*, *18*, 1896–1931.

Monier, C., Fournier, J., & Frégnac, Y. (2008). In vitro and in vivo measures of evoked excitatory and inhibitory conductance dynamics in sensory cortices. *J. Neurosci. Methods*, *169*, 323–365.

Paninski, L., Ahmadian, Y., Ferreira, D.G., Koyama, S., Rad, K. R., Vidne, M., et al. (2010). A new look at state-space models for neural data. *J. Comput. Neurosci.*, *29*, 107–126.

Pare, D., Shink, E., Gaudreau, H., Destexhe, A., & Lang, E. J. (1998). Impact of spontaneous synaptic activity on the resting properties of cat neocortical neurons in vivo. *J. Neurophysiol.*, *79*, 1450–1460.

Pham, J., Pakdaman, K., & Vibert, J.-F. (1998). Noise-induced coherent oscillations in randomly connected neural networks. *Phys. Rev. E*, *58*, 3610–3622.

Pospischil, M., Piwkowska, Z., Bal, T., & Destexhe, A. (2009). Extracting synaptic conductances from single membrane potential traces. *Neuroscience*, *158*, 545–552.

Ricciardi, L. M. (1976). Diffusion approximation for a multi-input model neuron. *Biol. Cybern.*, *24*, 237–240.

Ricciardi, L. M. (1977). *Diffusion processes and related topics in biology*. Berlin: Springer.

Rudolph, M., & Destexhe, A. (2003). Characterization of subthreshold voltage fluctuations in neuronal membranes. *Neural Comput.*, *15*, 2577–2618.

Rudolph, M., & Destexhe, A. (2005). An extended analytical expression for the membrane potential distribution of conductance-based synaptic noise. *Neural Comput.*, *17*, 2301–2315.

Rudolph, M., Piwkowska, Z., Badoual, M., Bal, T., & Destexhe, A. (2004). A method to estimate synaptic conductances from membrane potential fluctuations. *J. Neurophysiol.*, *91*, 2884–2896.

Rudolph, M., Pospischil, M., Timofeev, I., & Destexhe, A. (2007). Inhibition determines membrane potential dynamics and controls action potential generation in awake and sleeping cat cortex *J. Neurosci.*, *27*, 5280–5290.

Shadlen, M. N., & Newsome, W. T. (1995). Is there a signal in the noise? *Curr. Opin. Neurobiol.*, *5*, 248–250.

Shadlen, M. N., & Newsome, W. T. (1998). The variable discharge of cortical neurons: Implications for connectivity, computation, and information coding. *J. Neurosci.*, *18*, 3870–3896.

Shimokawa, T., & Shinomoto, S. (2009). Estimating instantaneous irregularity of neuronal firing. *Neural Comput.*, *21*, 1931–1951.

Shinomoto, S., Sakai, Y., & Funahashi, S. (1999). The Ornstein-Uhlenbeck process does not reproduce spiking statistics of neurons in prefrontal cortex. *Neural Comput.*, *11*, 935–951.

Smith, A. C., & Brown, E. N. (2003). Estimating a state-space model from point process observations. *Neural Comput.*, *15*, 965–991.

Softky, W. R., & Koch, C. (1993). The highly irregular firing of cortical cells is inconsistent with temporal integration of random EPSPs. *J. Neurosci.*, *13*: 334–350.

Stein, R. B. (1965). A theoretical analysis of neuronal variability. *Biophys. J.*, *5*, 173–194.

Tuckwell, H. C. (1988). *Introduction to theoretical neurobiology*, *vol. 2. Nonlinear and stochastic theories*. Cambridge: Cambridge University Press.

Vilela, R. D., & Lindner, B. (2009). Are the input parameters of white noise driven integrate and fire neurons uniquely determined by rate and CV? *J. Theor. Biol.*, *257*, 90–99.

Wehr, M., & Zador, A. M. (2003). Balanced inhibition underlies tuning and sharpens spike timing in auditory cortex. *Nature*, *426*, 442–446.

Received January 28, 2011; accepted May 24, 2011.